Coupled Systems Mechanics, *Vol. 14, No. 5 (2025) 431-450*
https://doi.org/10.12989/csm.2025.14.5.431

Analysis of interfacial stresses of composite bridge box steel-concrete beam

R. Benferhat[1,2], T. Hassaine Daouadji*[1,2], B. Abbes[3], T. Bensatallah[1,2], A. Rabahi[1,2] and F. Abbes[3]

[1]*Department of Civil Engineering, Ibn Khaldoun University of Tiaret, Algeria*
[2]*Laboratory of Geomatics and Sustainable Development LGéo2D, University of Tiaret, Algeria*
[3]*Laboratory Materials and Mechanical Engineering MATIM, University of Reims Cedex 2, France*

(Received April 25, 2025, Revised July 8, 2025, Accepted September 23, 2025)

Abstract. This study investigates the flexural reinforcement of composite box girder bridge decks through combined analytical and numerical approaches using ABAQUS software. The research focuses on deflection, interface stresses, and interfacial slip, while also examining the role of reinforcement type, adhesive properties, and the presence of deck openings. A comprehensive parametric study highlights that material selection, reinforcement configuration, and adhesive characteristics significantly affect structural performance. Moreover, deck openings are shown to increase interfacial stresses and slip due to stress concentration and redistribution.

Keywords: analytical and numerical analysis; composite box girder bridge decks; flexural reinforcement; interfacial slip; interfacial stresses

1. Introduction

Composite box girders, an important development in civil engineering, have been used in bridge construction since the 19th century. These robust and wide structural systems are suitable for road, highway, and railway crossings. Their torsional rigidity is ensured by hollow box sections, which provide exceptional resistance to twisting and enable the support of large spans. Assembly can be carried out either by launching or craning, offering both architectural flexibility and aerodynamic efficiency (Zhang *et al.* 2023, Bensatallah *et al.* 2024, Daouadji *et al.* 2025b, Zhu *et al.* 2025, Abdelaziz *et al.* 2025b, Rabahi *et al.* 2023).

Shi *et al.* (2021) investigated the flexural vibration characteristics of a variable cross-section box girder with corrugated steel webs, using a combination of the energy variational method and the extended spline finite point method. Wang *et al.* (2021) developed a computational framework to predict deflection in PC rigid-frame bridges with corrugated steel webs, based on the balanced cantilever method. Piotr (2024) analyzed the strengthening process of a classical steel-concrete composite beam. The beam consisted of a reinforced concrete slab connected by shear studs to an

*Corresponding author, Professor, E-mail: daouadjitahar@gmail.com

http://www.techno-press.org/?journal=csm&subpage=8 ISSN: 2234-2184 (Print), 2234-2192 (Online)

IPE steel profile. Ljubinković *et al.* (2019) examined the structural performance of curved steel panels to improve efficiency in steel and composite bridges, providing a detailed experimental program and relevant results for calibrating a numerical model. This model enables further exploration of the influence of several key parameters. Jiang *et al.* (2023) proposed a model to study the impact of critical parameters on bridges, grounded in the energy variational principle. They applied a finite difference method to investigate the shear lag effect and introduced a new definition of effective flange width. Sameera *et al.* (2015) studied the flexural behavior of steel-concrete composite beams strengthened with different types of connectors, combining full-scale experimental tests, push-out tests, and numerical and analytical analyses to evaluate the influence of the connectors, concrete, and grout on strength, stiffness, and interfacial slip. Abedin *et al.* (2022) analyzed twin steel box girder (TSBG) bridges following a girder fracture, developing a reliability analysis framework to evaluate structural redundancy and assess the remaining load-carrying capacity. Zhang *et al.* (2023) assessed the mechanical behavior of prefabricated composite box girders with corrugated steel webs through two rounds of internal prestressing tendon tensioning and a full-scale static load test at the Jialu River Bridge in Zhengzhou, China. Lee *et al.* (2015) studied the structural performance of prestressed composite girders with corrugated webs using five specimens, focusing on prestress level, tendon layout, welding methods, and shear connectors. Dong *et al.* (2019) combined experimental, numerical, and analytical approaches to investigate the flexural behavior of simply supported composite box girders with corrugated steel webs. Two 1:5 scale models of an actual bridge were built and tested, one using concrete-filled steel tubes and the other hollow steel tubes. Yan *et al.* (2020) developed an efficient numerical model for analyzing the flexural behavior of prestressed concrete steel girder (PCSG) structures, consisting of a hybrid beam-tendon element with three components: a concrete box girder segment element, a multi-node slipping tendon element, and a joint element, Main researchers have studied the application of this approach, we cite in this case (Daouadji *et al.* 2016, Bensatallah *et al.* 2021, Abdelaziz *et al.* 2025a, Daouadji 2017, Benferhat *et al.* 2023, Bouzid *et al.* 2024, Daouadji 2013, Radim *et al.* 2025, Rabahi *et al.* 2023).

Recent studies have extensively explored the strengthening and behavior of FRP and laminated composite plates. Daouadji *et al.* (2025a) developed refined theories to investigate the stability, vibration, and flexural response of composite plates on elastic foundations. Daouadji *et al.* (2025c) analyzed the influence of material properties, porosity, and shear deformation theories on the flexural and vibrational performance of composite plates. Benferhat *et al.* (2025) studied the effect of viscoelastic foundations and composite cores on thermo-mechanical and vibrational responses. Finally, Tounsi *et al.* (2008) proposed new deformation theories for laminated spherical shells, providing accurate solutions for modeling reinforced composite structures. These studies form an important basis for investigating FRP plate strengthening in bridges and composite beams. This study aims to enhance the understanding of composite box girder bridge decks by examining the impact of flexural reinforcement using composite materials. The analysis considers the presence or absence of deck openings and focuses on deflection, interface stresses, and interfacial slip. Analytical and numerical investigations are performed using ABAQUS software, while a parametric study highlights the influence of various parameters, including plate and adhesive properties, on the overall structural behavior.

2.1 Steel-concrete connection in composite box girder decks

Based on the relative slip at the interface of steel-concrete composite box girder bridge

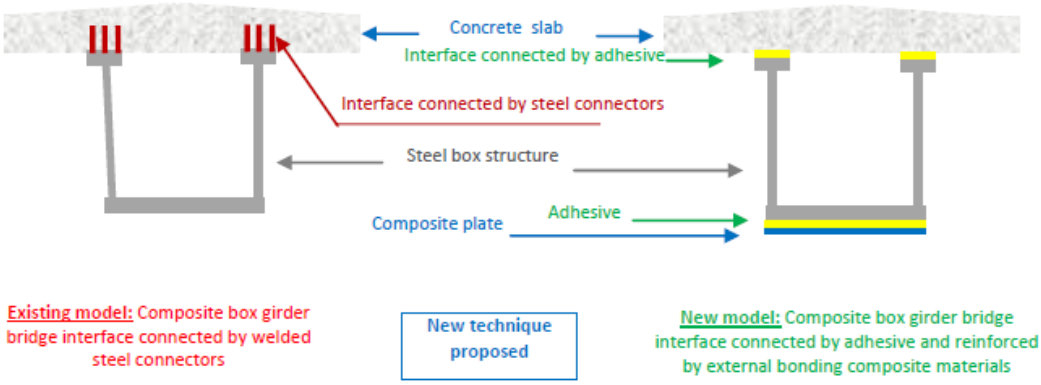

Fig. 1 Cross-section of a steel-concrete composite box girder deck with 90° web: mechanical connection (existing model) vs. adhesive bonding (proposed)

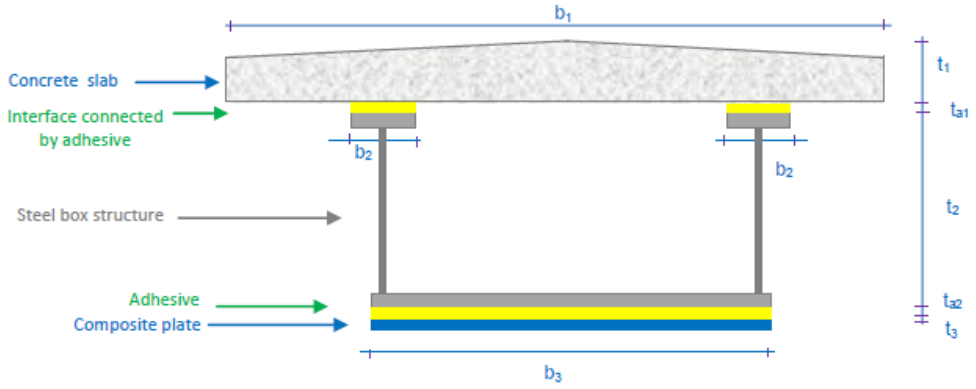

Fig. 2 Cross-section of the deck of a composite box girder bridge

connections with a perpendicular 90° core, it can be broadly classified as flexible or semi-rigid connections. Mechanical connectors, such as studs, which exhibit relatively higher slip, are considered flexible or semi-rigid, while adhesively bonded connections are regarded as rigid. Fig. 1 presents a schematic cross-sectional view comparing mechanically connected and adhesively bonded steel-concrete composite box girder bridge beams with a perpendicular 90° core. The behavior of steel-concrete composite connections has been widely investigated in several studies, with mechanical stud connectors being the most common solution. In contrast, adhesively bonded steel-concrete composite box girder bridge connections remain relatively new in civil engineering applications. Only a few studies have examined adhesively bonded connections over the past decade, which constitutes the focus of our research on composite box girder bridges.

2.2 Bridge description

The mixed-box girder bridge tested comprises a full concrete slab connected to a steel box girder, forming the bridge deck. The bridge was tested at full scale, with a slab 30 cm thick and 675 cm wide, connected to a steel box girder consisting of two upper flanges and two vertical webs (90°) joined by an unstiffened lower plate, as shown in Fig. 2. The bridge deck is designed to

- *Without openings:*

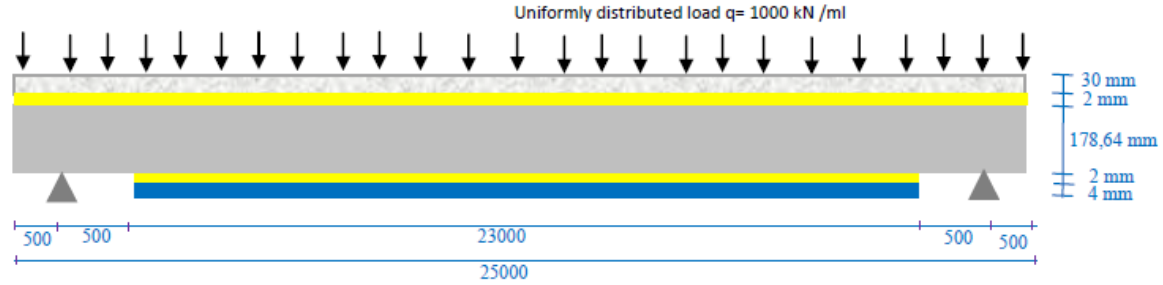

Fig. 3 Longitudinal section: Box girder at 90° without web openings

- *With openings:*

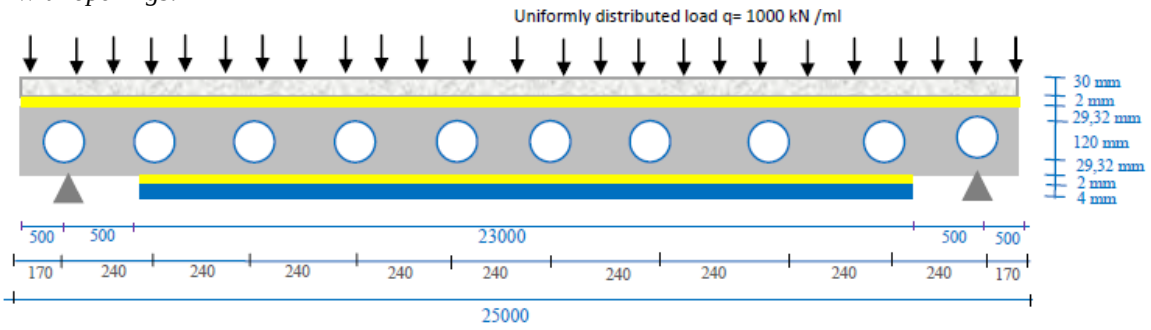

Fig. 4 Longitudinal section: Box girder at 90° with web openings

combine high strength, rigidity, and low weight, making it an efficient solution for bridge construction. This study aims to investigate the effect of flexural reinforcement using composite materials on the behavior of this mixed-box girder bridge deck, focusing on deflection, interfacial stresses, and slip, while considering the presence or absence of openings in the deck.

The reinforced concrete slab is assumed to be connected to the steel box girder through an adhesive layer and reinforced for flexural strength with a composite plate. The web of the steel box girder is analyzed both with and without openings.

3. The improved new technique's suppositions:

The transverse normal stress within the reinforced concrete slab and the composite box girder bridge is not considered in this analysis, instead, the focus is placed on the transverse shear stress and deformation in these components. The objective of the analytical method applied to concrete slabs reinforced with CFRP plates and bonded to steel beams (Figs. 3 and 4) is to provide a comparison with existing analytical models from the literature. This analytical approach is based on the following assumptions (Daouadji *et al.* 2024):

- ***Elastic Stress-Strain Relationship:*** Concrete, steel, CFRP plates, and adhesive are all assumed to follow an elastic stress-strain relationship.
- ***Simply Supported and Shallow Sections:*** The composite box girder bridge is assumed to be

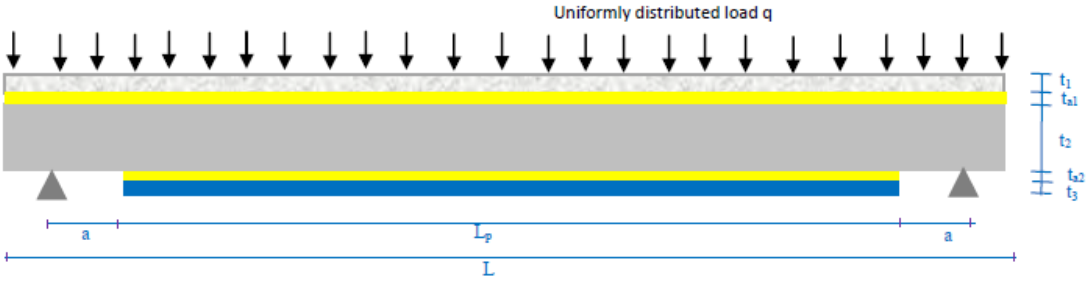

Fig. 5 Simply supported composite box girder bridge-slab reinforced concrete beam with perpendicular core 90 bonded by a composite plate

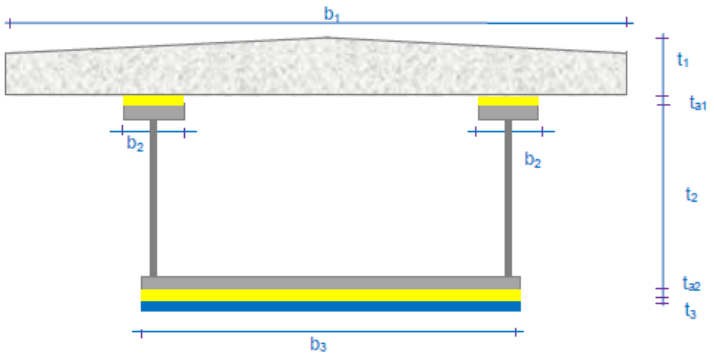

Fig. 6 Cross-section of the deck of a composite box girder bridge with perpendicular core 90

simply supported and shallow, ensuring that plane sections remain plane during bending.

- ***Imperfect Bond Between Concrete and Composite Girder:*** The bond between the concrete slab and the composite box girder bridge is imperfect, allowing for potential sliding between these two components.
- ***Perfect Bond Between CFRP Plate and Composite Girder:*** The bond between the CFRP plate and the composite box girder bridge is perfect, preventing any slip at the interface of the bond between the CFRP plate and the composite box girder bridge.
- ***Adhesive Role in Stress Transfer:*** The adhesive is considered to serve a single function in stress transfer, either from the concrete slab to the composite box girder bridge or from the CFRP plate to the composite box girder bridge.
- ***Constant Stress in Adhesive Layer:*** Stresses within the adhesive layer are assumed to be uniform across its thickness.
- ***Equal Curvatures Assumption:*** For the shear stress analysis, it is assumed that the curvatures of the composite box girder bridge and the CFRP plate are equal, allowing for the decoupling of shear and peel stress equations. However, this assumption does not apply to the normal stress solution, where vertical separation between the composite box girder bridge and the CFRP plate can occur when the beam is loaded.
- ***Parabolic Shear Deformation Distribution:*** A parabolic distribution of shear deformation is assumed through the depth of both the composite box girder bridge and the bonded CFRP plate.
- ***Bending Deformations:*** Bending deformations of both the composite box girder bridge and the CFRP plate are considered.

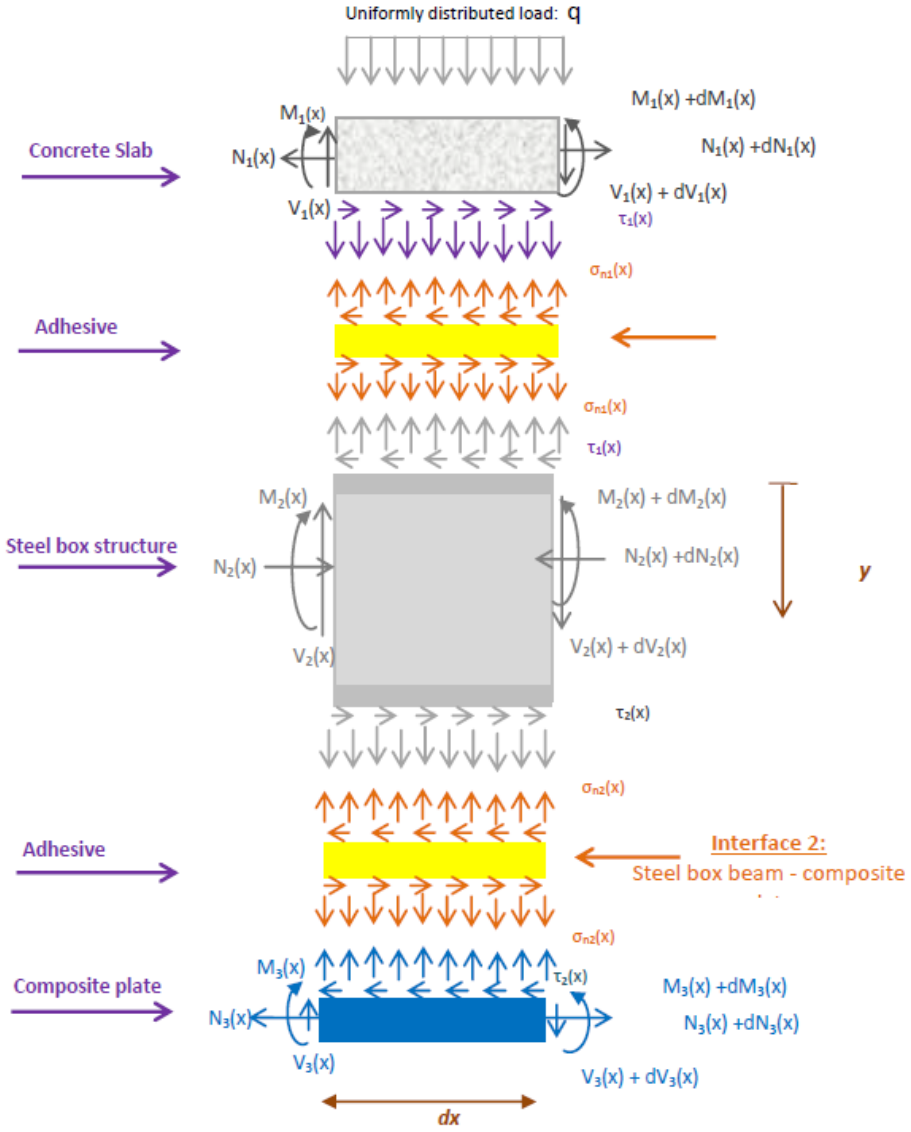

Fig. 7 Infinite forces in a composite box girder bridge reinforced with CFRP plate

3.1 Theoretical analysis

As shown in Figs. 5, 6, and 7, an infinitesimal element of length dx is considered from the CFRP-reinforced composite box girder bridge. The four main components of this system are steel, adhesive, concrete, and CFRP composite material. For this analysis, it is assumed that all these materials behave in a linear elastic manner.

Each material-steel, CFRP plate, and concrete plays a crucial role in resisting the moments and forces induced by the uniformly distributed transverse load q. Besides flexural and axial strains, the analysis also accounts for deformations due to potential interface slip. This approach ensures

an accurate and comprehensive assessment of the structural behavior under load.

3.1.1 Stress analysis at interface 1: Steel box girder-concrete slab

Shear stress distribution along the concrete slab-Steel box girder interface

According to Bensatallah *et al.* (2024), the interfacial shear stress's governing differential equation is as follows

$$\frac{d^2\tau(x)}{K_s \cdot dx^2} - K_1\left[\frac{(y_1+y_2)(y_1+y_2+t_{a1})}{E_1I_1+E_2I_2}+\frac{1}{E_1A_1}+\frac{1}{E_2A_2}\right]\frac{d\tau(x)}{dx}+K_1\frac{(y_1+y_2)}{E_1I_1+E_2I_2}\cdot V_T(x)=0 \quad (1)$$

Where

$$K_1=\left[\frac{t_{a1}}{G_{a1}}+\frac{t_1}{3G_1}+\frac{t_2}{3G_2}\xi\right]^{\frac{-1}{2}} \quad (2)$$

$$\xi=\frac{b_2(t_2-t_0)^3-t_0^3-t_2^3+6t_2^2t_0)}{6G_2t_2A_2}+\frac{b_0(3t_{a1}^2(t_2-2t_0)-(t_2-t_0)^2+t_0^2)}{6G_2t_2A_2} \quad (3)$$

For simplicity, the general solutions presented below are limited to loading which is either concentrated or uniformly distributed over part or the whole span of the beam, or both. For such loading, $d^2V_T(x)/dx^2=0$, and the general solution to Eq. (1) is given by simplified form

$$\tau(x)=\alpha_1e^{\delta\cdot x}+\alpha_2e^{-\delta\cdot x}+\frac{K_1}{\delta^2}\left(\frac{1}{E_1A_1}+\frac{1}{E_2A_2}\right).V_T(x) \quad (4)$$

Where

$$\delta=\left[\frac{b_2\left[\frac{(y_1+y_2)(y_1+y_2+t_{a1})}{E_1I_1+E_2I_2}+\frac{1}{E_1A_1}+\frac{1}{E_2A_2}\right]}{\frac{t_{a1}}{G_{a1}}+\frac{t_1}{3G_1}+\frac{t_2}{3G_2}\xi}\right]^{\frac{1}{2}} \quad (5)$$

α_1 and α_2 constant coefficients determined from the boundary conditions.

***The interfacial shear stress for this uniformly distributed load*:** For $0 \le x \le L$ p at any point is written as

$$\tau(x)=\left(\frac{t_2a(L-a)}{2E_2I_2\left(\frac{t_{a1}}{G_{a1}}+\frac{t_2}{3G_2}\xi\right)}-\frac{t_1+t_2}{2\delta^2(E_2I_2+E_1I_1+b_1)}\right)\frac{qe^{-\delta x}}{\delta}+\frac{t_1+t_2}{2\delta^2(E_2I_2+E_1I_1+b_1)}q\left(\frac{L}{2}-a-x\right) \quad (6)$$

Where q is the uniformly distributed load and x, a, L and L_p are defined in Figs. 2, 3 and 4.

Interfacial shear stress for a single point load: For as $0 \le x \le \frac{L}{2}$ as

$$\tau(x)=\left[\frac{\frac{1}{E_1A_1}+\frac{1}{E_2A_2}}{b_2\left[\frac{(y_1+y_2)(y_1+y_2+t_{a1})}{E_1I_1+E_2I_2}+\frac{1}{E_1A_1}+\frac{1}{E_2A_2}\right]}\right]\left[\frac{(e^{-\delta\cdot\frac{L}{2}+\delta\cdot x}-e^{\delta\cdot\frac{L}{2}-\delta\cdot x})}{e^{-\delta\cdot\frac{L}{2}}+e^{\delta\cdot\frac{L}{2}}}+1\right]\frac{P}{2} \tag{7}$$

Where P is the single point load and x, a, L and L_p are defined in Figs 2, 3 and 4.

Slip distribution along the steel-concrete interface

As noted in the assumptions, the slip of adhesive is proportional to the shear force, which the connector transmitted, and after resolution of governing differential equation for the slip strain at the interface of uniformly distributed load is calculated as Bensatallah *et al.* (2024), the slip distribution along the steel-concrete interface in the adhesive can be expressed as follows

$$S(x)=\frac{t_{a1}}{G_{a1}}(\alpha_1e^{\delta\cdot x}+\alpha_2e^{-\delta\cdot x}+\frac{K_1}{\delta^2}(\frac{1}{E_1A_1}+\frac{1}{E_2A_2}).V_T(x)) \tag{8}$$

Where $S(x)$ represent slip between adhrends and $K_s=G_{a1}/t_{a1}$ is shear stiffness of the adhesive, G_{a1} and t_{a1} are shear modulus and thickness of the adhesive.

Slip interfacial for a single point load: For the case of simply supported beams with a single load, the slip due to load is

$$S(x)=\frac{P}{2}\left[\frac{\frac{1}{E_1A_1}+\frac{1}{E_2A_2}}{b_2\left[\frac{(y_1+y_2)(y_1+y_2+t_{a1})}{E_1I_1+E_2I_2}+\frac{1}{E_1A_1}+\frac{1}{E_2A_2}\right]}\right]\left[\frac{e^{-\delta\cdot\frac{L}{2}+\delta\cdot x}}{(e^{-\delta\cdot\frac{L}{2}}+e^{\delta\cdot\frac{L}{2}})}-\frac{\delta\cdot P\cdot e^{\delta\cdot\frac{L}{2}-\delta\cdot x}}{2(e^{-\delta\cdot\frac{L}{2}}+e^{\delta\cdot\frac{L}{2}})}+1\right] \tag{9}$$

3.1.2. Stress analysis at interface 2: Steel box girder - composite plate

Shear stress distribution along the CFRP plate - Steel box girder interface

The governing differential equation for the interfacial shear stress is expressed as (Daouadji *et al.* 2024)

$$\frac{d^2\tau(x)}{dx^2}-\frac{A_{11}^{'}+\frac{b_3}{E_2A_2}+\frac{(t_2+t_3)(t_2+t_3+2t_{a2}).b_3D_{11}^{'}}{2(E_1I_1D_{11}^{'}+b_2)}}{\frac{t_{a2}}{G_{a2}}+\frac{t_2}{3G_2}\eta}\tau(x)+\frac{\frac{(t_2+t_3)D_{11}^{'}}{E_2I_2D_{11}^{'}+b_3}}{2(\frac{t_{a2}}{G_{a2}}+\frac{t_2}{3G_2}\eta)}V_T(x)=0 \tag{10}$$

Where η is a geometrical coefficient which is given as

$$\eta=b_2\frac{\left(-t_0^3+6t_0t_2^2-t_2^3+(t_2-t_0)^3\right)}{2A_2t_2^2}+b_0\frac{\left(3t_2^2(t_2-2t_0)-(t_2-t_0)^3+t_0^3\right)}{2A_2t_2^2} \tag{11}$$

When η=1, it matches the same expression provided by Daouadji (2024). Nonetheless, it was observed that in the case of the box girder beam section, there were: 1. In the interest of simplicity, the general solutions that follow are restricted to loading that is either uniformly distributed over

the entire beam, a portion of it, or both (Fig. 4). When loading is such that $d^2V_T(x)/dx^2=0$, the general solution to Eq. (12) is as follows

$$\tau(x)=\alpha_3\cosh(\mu x)+\alpha_4\sinh(\mu x)+\left(\frac{(t_2+t_3)D_{11}^{'}}{4\mu^2(E_2I_2D_{11}^{'}+b_3)\left(\frac{t_{a2}}{G_{a2}}+\frac{t_2}{3G_2}\eta\right)}\right)V_T(x) \tag{12}$$

where γ is given as

$$\mu=\left[\frac{A_{11}^{'}+\frac{b_3}{E_2A_2}+\frac{(t_2+t_3)(t_2+t_3+2t_{a2}).b_3D_{11}^{'}}{2(E_2I_2D_{11}^{'}+b_3)}}{\frac{t_{a2}}{G_{a2}}+\frac{t_2}{3G_2}\eta}\right]^{\frac{1}{2}} \tag{13}$$

Where the constant coefficients, α_3 and α_4, are ascertained from the boundary conditions. A simply supported box girder beam that is subjected to a uniformly distributed load has been examined in this study (Fig. 5). According to Daouadji *et al.* (2024), the interfacial shear stress for this uniformly distributed load at any given point is expressed as follows

$$\tau(x)=\left(\frac{t_2a(L-a)}{2E_2I_2\left(\frac{t_{a2}}{G_{a2}}+\frac{t_2}{3G_2}\eta\right)}-\frac{(t_2+t_3)D_{11}^{'}}{2\mu^2(E_2I_2D_{11}^{'}+b_3)}\right)\frac{qe^{-\mu x}}{\mu}++\frac{t_2+t_3}{2\mu^2(E_2I_2D_{11}^{'}+b_3)}D_{11}^{'}q\left(\frac{L}{2}-a-x\right) \tag{14}$$

$$0\le \mathrm{x}\le \mathrm{L_P}$$

Where x, a, L, and L_p are defined in Figs. 2, 3 and 4, and q is the uniformly distributed load. As illustrated in Fig. 5, a simply supported box girder beam underwent investigation and was subjected to a concentrated load P at mid-span. For this load case, the interfacial shear stress at any given point is expressed as follows:

The reinforced zone contains the concentrated load P.

$$\tau(x)=\frac{a.t_2}{2E_2I_2\mu\left(\frac{t_{a2}}{G_{a2}}+\eta\frac{t_2}{3G_2}\right)}Pe^{-\mu x}+\left(\frac{(t_2+t_3)D_{11}^{'}}{\left(\frac{t_{a2}}{G_{a2}}+\eta\frac{t_2}{3G_2}\right)(E_2I_2D_{11}^{'}+b_3)2\mu^2}\right)P\cosh(\mu x)e^{-\mu\left(\frac{l}{2}-a\right)} \tag{15}$$

The concentrated load P is positioned in the not reinforced zone

$$\tau(x)=\frac{t_2}{2E_2I_2\mu\left(\frac{t_{a_2}}{G_{a2}}+\eta\frac{t_2}{3G_2}\right)}Pb_2e^{-\mu x} \tag{16}$$

Where P is the concentrated load and x, a, L and L_p are defined in Figs. 2, 3 and 4.

Normal stress distribution along the CFRP plate-Steel box girder interface under evenly distributed load

As noted in the assumptions, the interfacial normal stress of adhesive is proportional to the shear force, and after resolution of governing differential equation for the interfacial normal stress strain at the interface of uniformly distributed load is calculated as Daouadji *et al.* (2024), the

interfacial normal stress distribution along the steel-composite interface in the adhesive can be expressed as follows

$$\sigma_n(x) = e^{-\beta x}\left[\alpha_5 \cos(\beta x) + \alpha_6 \sin(\beta x)\right] - \left(\frac{y_2 b_3 - \frac{D_{11}^{'} E_2 I_2 t_3}{2}}{D_{11}^{'} E_2 I_2 + b_3}\right)\frac{d\tau(x)}{dx} - \frac{1}{D_{11}^{'} E_2 I_2 + b_3} q \tag{17}$$

Where

$$\boldsymbol{\beta} = \left[\frac{\boldsymbol{E_{a2}}}{\boldsymbol{4t_{a2}}}\left(\boldsymbol{D_{11}^{'}} + \frac{\boldsymbol{b_3}}{\boldsymbol{E_2 I_2}}\right)\right]^{\frac{1}{4}} \tag{18}$$

As is described by Daouadji (2024), the constants α_5 and α_6 in Eq. (17) are determined using the appropriate boundary conditions and they are written as follows

$$\alpha_5 = \frac{\frac{E_{a2}}{t_{a2}}\left[V_T(0) + \beta M_T(0)\right]}{2\beta^3 E_2 I_2} - \frac{b_3 \frac{E_{a2}}{t_{a2}}\left(\frac{y_2}{E_2 I_2} - \frac{D_{11}^{'} t_3}{2b_3}\right)}{2\beta^3}\tau(0) + \frac{\left[\frac{d^4\tau(0)}{dx^4} + \beta\frac{d^3\tau(0)}{dx^3}\right]}{2\beta^3} \tag{19}$$

$$\alpha_6 = -\frac{\frac{E_{a2}}{t_{a2}}\frac{M_T(0)}{E_2 I_2} - \left[\frac{y_2 b_3 - \frac{D_{11}^{'} E_2 I_2 t_3}{2}}{D_{11}^{'} E_2 I_2 + b_3}\right]\frac{d^3\tau(0)}{dx^3}}{2\sqrt{\frac{E_{a2}}{4t_{a2}}(0)\left(D_{11}^{'} + \frac{b_3}{E_2 I_2}\right)}} \tag{20}$$

The bending moment $M_T(0)$ and shear force $V_T(0)$ at the end of the soffit plate are still used in the above expressions for the constants α_5 and α_6. Eq. (17) can then be used to find the interfacial normal stress after the constants α_5 and α_6 have been established.

3.2 Finite element analysis

A finite element model of the bridge was created using ABAQUS software to replicate local and overall behaviors. The model uses a multi-linear inelastic material model with isotropic hardening to accurately depict the response of steel plates, diaphragms, and reinforcement under various loads. This comprehensive analysis provides insights into the bridge's mechanical behavior and performance under different box girder deck configurations. The study uses ABAQUS software to analyze the caisson bridge, determining deflection and interface stresses under various reinforcement scenarios. A three-dimensional finite element (3D FE) model was developed to account for the geometric and nonlinear material behavior of steel composite beams. The Von Misses yield criterion was adopted for nonlinear analysis. The eight-node brick element S4R was used to model the box girder bridge. A finite element model was developed using ABAQUS to evaluate stresses in reinforced beams and adhesives, reducing computational effort.

4. Results and discussion

Table 1 Characteristics of the materials used

Component	Width (mm)	Depth (mm)	Young's modulus (MPa)	Poisson's ratio
Concrete slab	6750	300	E_b=30000	0.18
steel box beam	3000	/	E_a=210000	0.3
Adhesive layer	b_1=2650	t_a=2	E_a=3000	0.35
CFRP	b_2=2650	t_2=4	$E2$= 40 000	0.28
GFRP	b_2=2650	t_2=4	$E2$=73 000	0.22
Carbodur	$b2$=2650	t_2=4	$E2$=165 000	0.3
4-ply fabric	$b2$=2650	t_2=4	$E2$=230 000	0.3

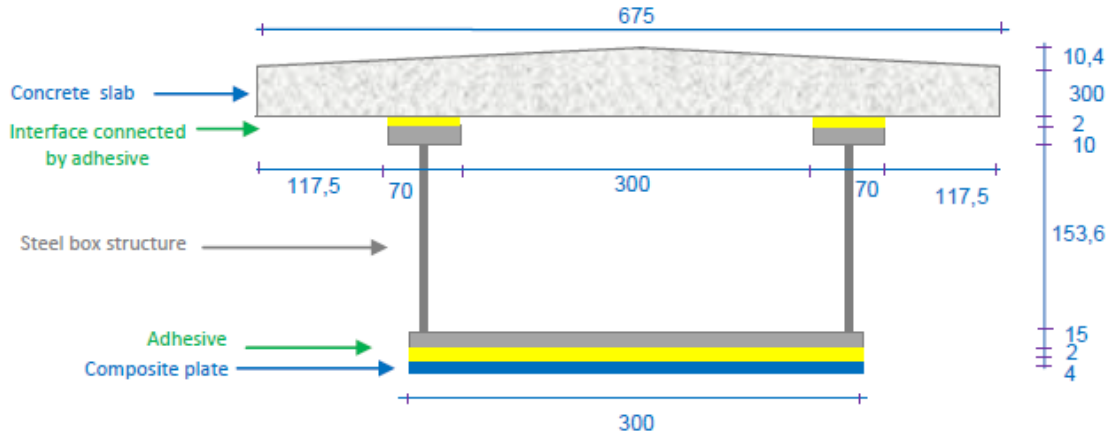

Fig. 8 Geometric characteristic of a cross-section of the deck of a composite box girder bridge with perpendicular core 90

This section presents the numerical and analytical investigation of the flexural behavior of reinforced steel box beams. The objective is to evaluate interfacial stresses and slip in box beams with and without openings. The bridge span has a length of L=25,000 mm (25 m), subjected to a uniformly distributed load of q=1000 kN/m, and is reinforced with a composite plate that includes an unreinforced length of a=500 mm. The material properties used in this study are summarized in Table 1 and illustrated in Figs. 3, 4, and 8.

4.1 Analytical results

Fig. 9 illustrates the variation in deflection of a composite-reinforced steel box beam under flexure for different web inclinations. The x-axis represents the inclination angle, ranging from 50° to 90°, while the y-axis represents the deflection, ranging from 2.5 to 5.5 cm. The results show that as the inclination angle increases, the beam deflection decreases. This indicates that a box beam with a 90° web inclination can sustain higher loads.

Fig. 10 presents a comparison of interface stresses (both normal and shear) in box girder beams, with and without openings, with the Daouadji 2024 model, plotted as a function of distance (X) in millimeters. The graph reveals that interface stresses are higher in box girder beams with openings in contrast to those without openings. This difference is most noticeable at the openings

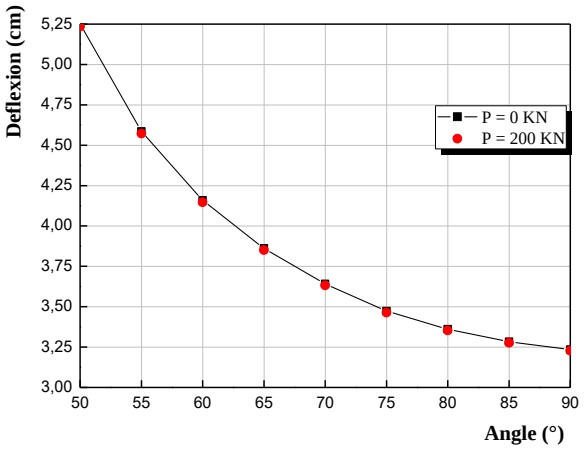

Fig. 9 Variation of the deflection of a steel box beam reinforced with composite in flexion according to various inclination angles

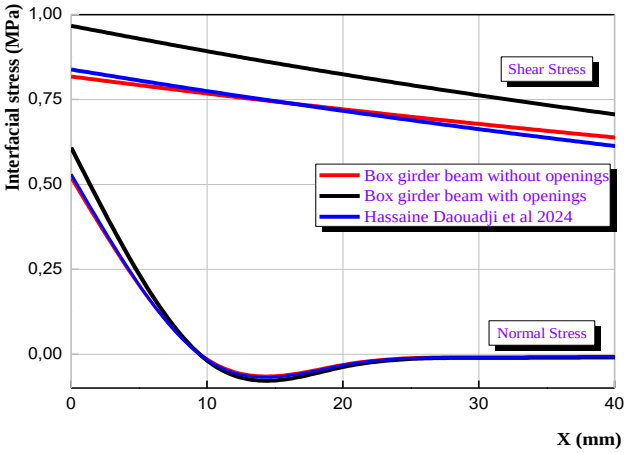

Fig. 10 Comparison of interfacial stresses in box girder beams with and without openings to the Daouadji 2024 model

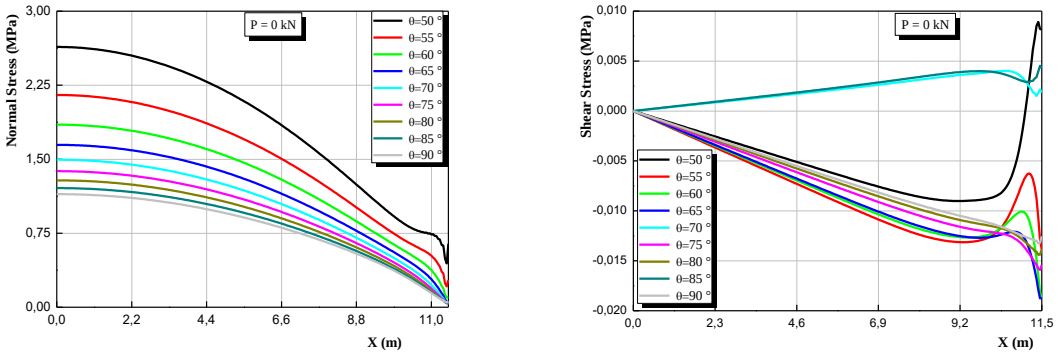

Fig. 11 Effect of composite plate stiffness on interfacial stresses of a box girder beam with and without openings reinforced in flexure by a hybrid plate

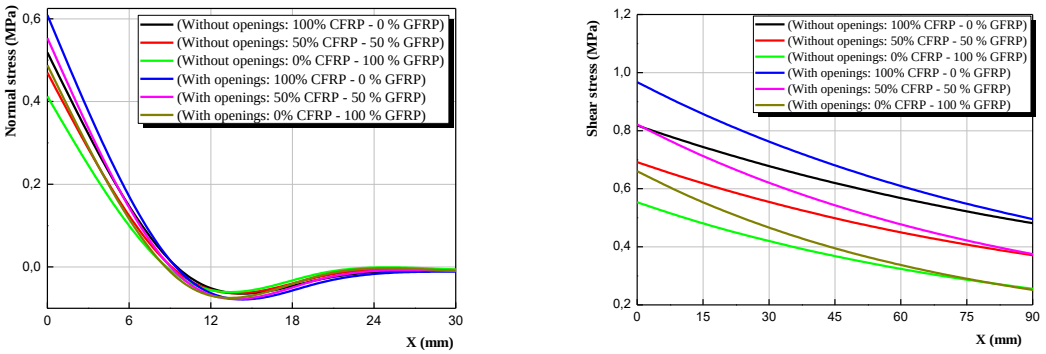

Fig. 12 Effect of composite plate stiffness on interfacial stresses of a box girder beam with and without openings reinforced in flexure by a hybrid plate

Table 2 Impact of adhesive stiffness on interfacial stresses in box girder beams, both with and without openings, reinforced in flexure using a variety of composite plates

		CFRP (2 layers)		50 % CFRP/50% GFRP		GFRP (2 layers)	
	E_a (MPa)	τ	σ	τ	σ	τ	σ
Without openings	5000	0.824459	0.595856	0.697366	0.539929	0.558036	0.474234
	10000	0.829465	0.716291	0.701707	0.649282	0.561616	0.570556
	15000	0.831160	0.796545	0.703178	0.722130	0.562829	0.634695
	20000	0.832012	0.858539	0.703916	0.778388	0.563438	0.684216
	30000	0.832525	0.953814	0.704658	0.864838	0.564049	0.760296
With openings	5000	0,97948	0,70309	0,83181	0,84559	0,66888	0,56405
	10000	0,98891	0,84847	0,83999	0,77198	0,67562	0,68144
	15000	0,99212	0,94482	0,84277	0,85981	0,67792	0,68144
	20000	0,99374	1,01905	0,84418	0,92747	0,67908	0,81904
	30000	0,99537	1,08031	0,84559	1,03123	0,68025	0,91084

and diminishes gradually along the remaining span of the beam. Fig. 11 illustrates the effect of varying the inclination angle of the webs of the reinforced steel box beam under flexure on the interface stresses. The inclination angle of the webs ranges from θ=50 to 90°. It is noteworthy that varying the inclination angle of the webs significantly affects both normal and shear stresses.

Fig. 12 illustrates the impact of the composite reinforcement plate type on the interface stresses of a mixed box girder bridge with and without openings, subjected to a uniformly distributed load, with interface stresses plotted as a function of the position (x) in millimeters. The normal and shear stress curves shows that the stresses are lowest for hybrid plates, both for the bridge with openings and for the bridge without openings. This is due to the combination of carbon and aluminum properties, which enables the hybrid plate to be both lightweight and strong. The stresses are higher for CFRP and GFRP plates, in that order.

Table 2 presents the influence of adhesive stiffness on the interface stresses of steel box girder beams, with and without openings, reinforced in flexure by different types of composite plates. A slight increase in normal stresses is observed as the adhesive stiffness increases from 5,000 MPa to 15,000 MPa. Beyond 15,000 MPa, normal stress remain nearly constant. Shear stresses show a greater increase compared to normal stresses with increasing adhesive stiffness. An increase of

Table 3 Influence of adhesive layer thickness (t_a) on interface stresses in box girder beams, whether or not they have openings, and reinforced in flexure with various composite plates

		CFRP (2 layers)		50 % CFRP/50% GFRP		GFRP (2 layers)	
	t_a (mm)	τ	σ	τ	σ	τ	σ
Without openings	1	0,82613	0,62569	0,69881	0,56703	0,55922	0,49810
	2	0,81796	0,51849	0,69173	0,46965	0,55339	0,41228
	3	0,81009	0,46275	0,68491	0,41899	0,54776	0,36761
	4	0,80250	0,42580	0,67832	0,38540	0,54233	0,33798
With openings	1	0,98259	0,73921	0,83451	0,67236	0,67110	0,59323
	2	0,96739	0,60890	0,82133	0,55348	0,66023	0,48792
	3	0,95301	0,54047	0,80886	0,49103	0,64995	0,43257
	4	0,93937	0,49481	0,79702	0,44935	0,64019	0,39561

Table 4 Effect of Poisson's ratio of the adhesive on interfacial stresses in box girder beams with and without openings, strengthened in flexure with various composite plates

		CFRP (2 layers)		50 % CFRP/50% GFRP		GFRP (2 layers)	
	υ_a	τ	σ	τ	σ	τ	σ
Without openings	0,3	0,81855	0,51885	0,69224	0,46998	0,55381	0,41259
	0,35	0,81796	0,51848	0,69173	0,46965	0,55339	0,41228
	0,4	0,81737	0,51812	0,69121	0,46932	0,55296	0,41198
	0,45	0,81677	0,51776	0,69070	0,46898	0,55254	0,41168
	0,5	0,81618	0,51740	0,69019	0,46865	0,55212	0,41138
With openings	0,3	0,96849	0,60955	0,82228	0,55409	0,66102	0,48847
	0,35	0,96740	0,60889	0,82133	0,55348	0,66023	0,48792
	0,4	0,96631	0,60824	0,82038	0,55288	0,65945	0,48737
	0,45	0,96522	0,60758	0,81944	0,55227	0,65867	0,48682
	0,5	0,96413	0,60693	0,81850	0,55166	0,65790	0,48628

approximately 25% and 40% in shear stresses is noted between 5,000 MPa and 30,000 MPa for box girder beams without and with openings, respectively.

Table 3 illustrates the impact of adhesive layer thickness on the interface stresses in composite box beams, with or without openings, reinforced in flexure with different composite plates. The results are presented for two types of interface stresses: normal and shear. Normal stresses progressively decrease as the adhesive layer thickness increases. This decrease is more pronounced for beams without openings than for those with openings. Conversely, shear stresses show a slight increase with increasing adhesive thickness. This increase is more pronounced for beams without openings than for those with openings.

Table 4 presents the impact of Poisson's ratio on the interfacial stresses in composite box beams, with and without openings, reinforced in flexure with three types of composite plates: CFRP, 50% CFRP/50% GFRP, and 50% GFRP/50% CFRP. Interfacial stresses slightly increase with Poisson's ratio, and this effect becomes more pronounced at higher values of ν. Interfacial stresses are generally higher in beams with openings.

Fig. 13 illustrates the variation of interfacial slip in a box beam subjected to a uniformly distributed load, for two configurations: with and without openings. Beams reinforced with CFRP

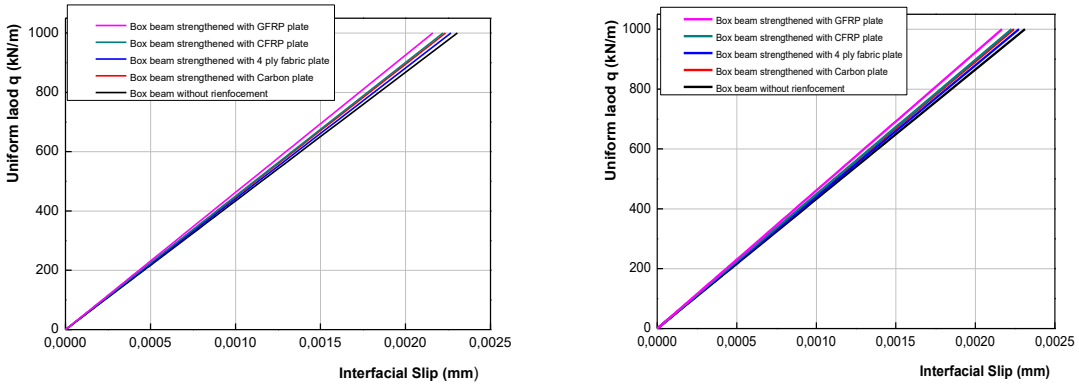

Without openings With openings

Fig. 13 Variation of interfacial slip in a box girder beam with different types of reinforcement as a function of uniformly distributed loading

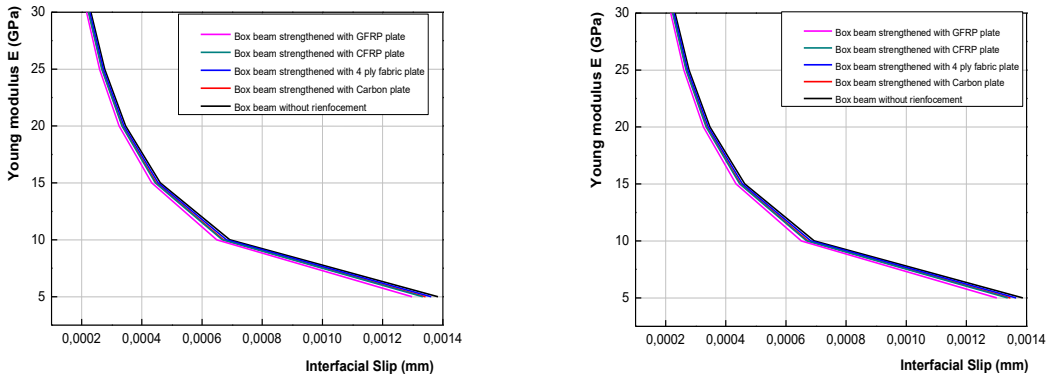

Without openings With openings

Fig. 14 Effect of Young's modulus (*E*) of adhesive on the interfacial slip of a box girder beam reinforced by different types of reinforcement plates, under uniformly distributed loading

plates exhibit the lowest interfacial slip, followed by those with 50% CFRP/50% GFRP mixed plates, and finally those with GFRP. This behavior is explained by the mechanical properties of the reinforcement materials, as CFRP is stiffer and stronger than GFRP. Interfacial slip increases significantly in box beams with openings, as stress concentrations around the openings weaken the structure and increase the demand on the adhesive layer between the reinforcement and the beam.

Fig. 14 shows the stiffness of reinforced box beams with different composite plates under a uniformly distributed load, highlighting several trends. The greatest stiffness is generally observed in beams reinforced with CFRP plates, followed by those with CFRP/GFRP mixed plates, and finally those with GFRP plates. The presence of openings significantly reduces stiffness, as stresses are concentrated around them. Additionally, interfacial slip decreases as the adhesive Young's modulus increases, particularly in beams with openings.

Fig. 15 illustrates the impact of the adhesive's Poisson's ratio on the interfacial slip of box beams reinforced with various composite plates, subjected to a uniformly distributed load. Interfacial slip decreases with increasing adhesive Poisson's ratio, effectively enhancing the

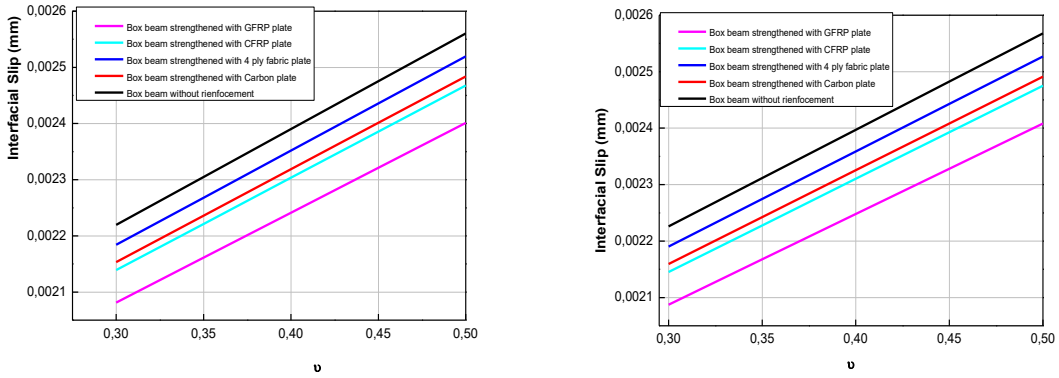

Without openings With openings

Fig. 15 Effect of Poisson coefficient (υ) of the adhesive on the interfacial slip of a box girder beam reinforced by different types of reinforcement plates, under uniformly distributed loading

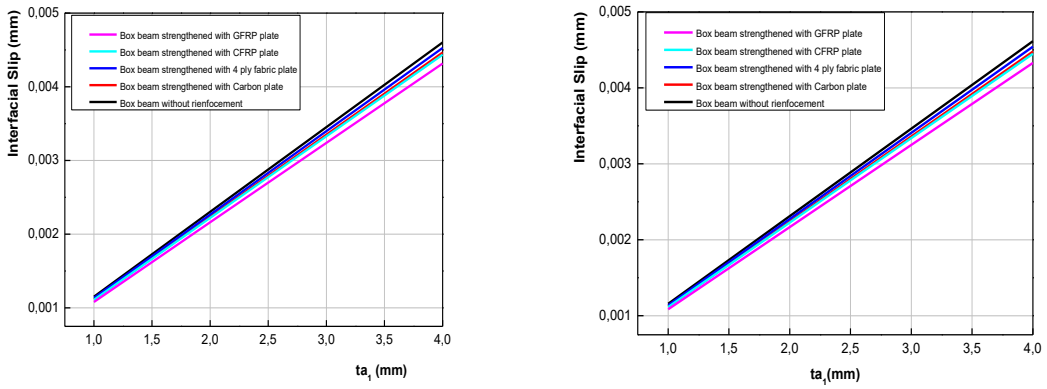

Without openings With openings

Fig. 16 Effect of adhesive thickness (t_{a1}) on the interfacial slip of a box girder beam reinforced by different types of reinforcement plates, under uniformly distributed loading

adhesive's stiffness. Beams reinforced with CFRP, GFRP, and 4-ply fabric plates exhibit the lowest interfacial slip due to their higher rigidity. In the presence of openings, interfacial slip becomes more significant due to stress concentrations

Fig. 16 illustrates the influence of adhesive relative thickness on the interfacial slip of box beams reinforced with various composite plates, with and without openings. The results show that interfacial slip decreases as adhesive thickness increases. The reduction is most pronounced for 4-ply fabric plates, followed by GFRP and CFRP plates without openings. This trend persists in beams with openings, where the largest variation is observed for 4-ply fabric plates, highlighting the detrimental effect of openings on the ability of reinforcement plates to transfer loads effectively.

4.2 Numerical results:

Fig. 17 shows the relationship between transverse and longitudinal interfacial slip of a

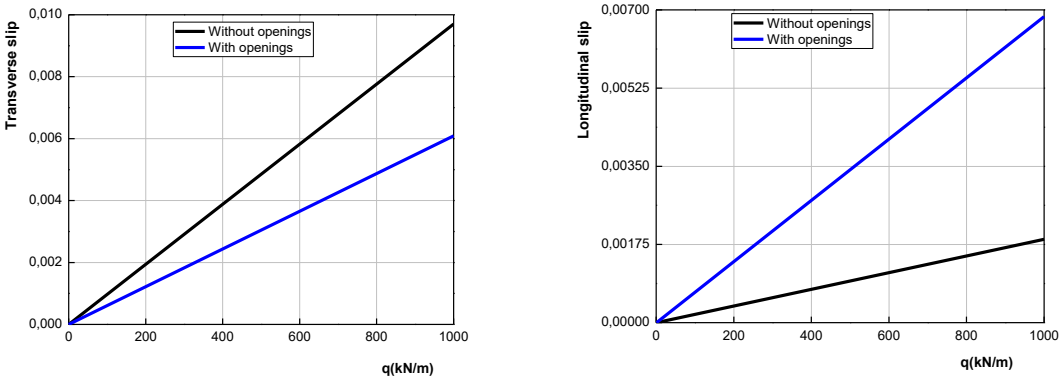

Fig. 17 Interfacial slip of the deck of a composite box girder bridge with and without openings subjected to a uniformly distributed load

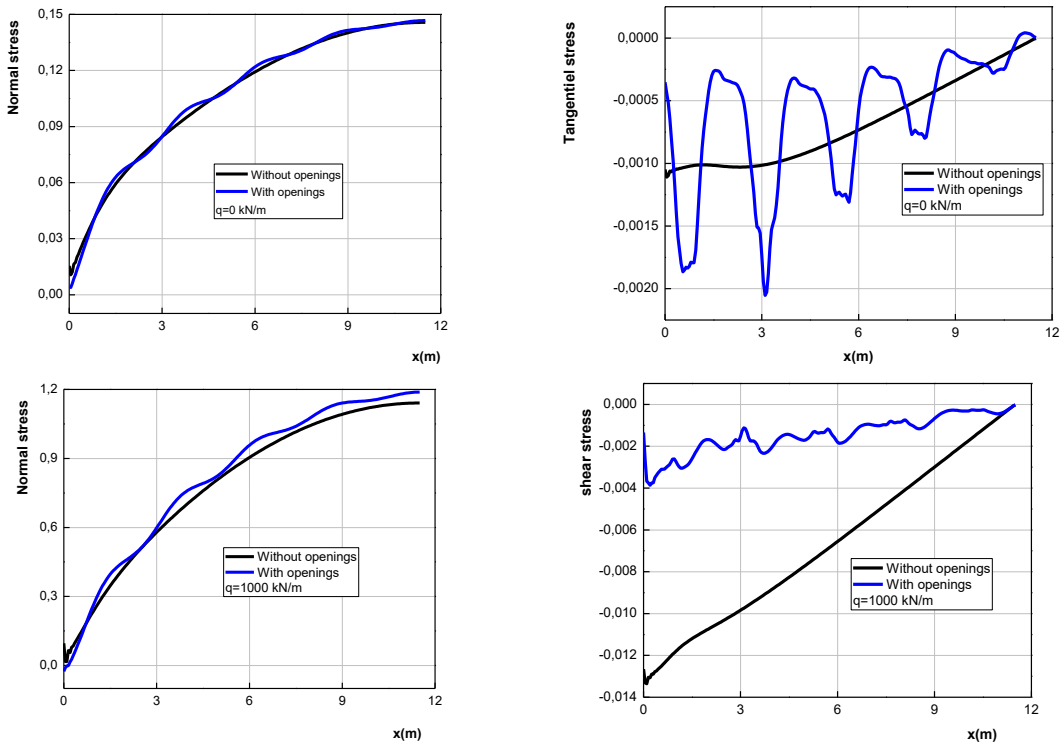

Fig. 18 Interfacial stress of the deck of a composite box girder bridge with and without openings subjected to a uniformly distributed load

composite box girder bridge, with and without openings, subjected to a uniformly distributed load as a function of the applied load (q) in kN/m. The results indicate that deck slip is more pronounced in the bridge with openings than in the one without, due to stress redistribution induced by the openings. However, the influence of openings is less significant on longitudinal slip than on transverse slip.

Fig. 18 illustrates the variation of interface stresses (normal and shear) in a composite box girder bridge, with and without openings, subjected to a uniformly distributed load, plotted against position (x) in meters. The results show that interface stresses are higher in the bridge with openings than in the one without. However, the influence of openings is less significant on shear stresses than on normal stresses. Furthermore, interface stresses reach their maximum at midspan, exceeding those at the edges, particularly under higher loads than under lower ones.

5. Conclusions

This study investigates flexural reinforcement strategies for mixed-box girder bridge decks, with a focus on interfacial stresses and slip. A comprehensive analytical and numerical analysis is conducted using ABAQUS software, complemented by a parametric study to assess the effects of material properties, reinforcement type, adhesive characteristics, and deck openings on structural performance. The findings indicate that material selection, reinforcement configuration, and adhesive properties significantly influence interfacial stresses and slip. Furthermore, the presence of openings in box girder decks leads to elevated interfacial stresses and increased slip, due to stress concentration and redistribution.

References

Abderezak, R., Daouadji, T.H. and Rabia, B. (2022), "Analysis and modeling of hyperstatic RC beam bonded by composite plate symmetrically loaded and supported", *Steel Compos. Struct.*, **45**(4), 591-603. https://doi.org/10.12989/scs.2022.45.4.591.

Abderezak, R., Daouadji, T.H. and Tayeb, B. (2023), "Composite aluminum-slab RC beam bonded by a prestressed hybrid carbon-glass composite material", *Struct. Eng. Mech.*, **85**(5), 573-592. https://doi.org/10.12989/sem.2023.85.5.573.

Abedin, M., Mehrabi, A.B., Azizinamini, A., Ghosn, M., Nowak, A.S. and Babu, A.R. (2022), "Reliability evaluation of twin steel box girder bridges using a simplified method", *Eng. Struct.*, **259**, 114122. https://doi.org/10.1016/j.engstruct.2022.114122.

Bensattalah, T. and Daouadji, T.H. (2024), "Analysis of I-steel-concrete beam bonded with an glue under shock load: effect of slip and deflection", *Hydraulic and Civil Engineering Technology IX*, 411-420.

Bouzid, H., Idriss, R., Rabia, B. and Daouadji, T.H. (2024), "Strengthening reinforced concrete beams: A comparative study of NSM and EB FRP systems using Cast3m software and theoretical analysis", *Struct. Eng. Mech.*, **92**(6), 547-557. https://doi.org/10.12989/sem.2024.92.6.547.

Chen, Y., Dong, J., Tong, Z., Jiang, R. and Yue, Y. (2020), "Flexural behavior of composite box girders with corrugated steel webs and trusses", *Eng. Struct.*, **209**, 110275. https://doi.org/10.1016/j.engstruct.2020.110275.

Daouadji, T.H., Abderezak, R. and Rabia, B. (2024), "Analysis of mechanical performance of continuous steel beams with variable section bonded by a prestressed composite plate", *Steel Compos. Struct.*, **50**(2), 183-199. https://doi.org/10.12989/scs.2024.50.2.183.

Daouadji, T.H. (2013), "Analytical analysis of the interfacial stress in damaged reinforced concrete beams strengthened by bonded composite plates", *Strength Mater.*, **45**(5), 587-597. https://doi.org/10.1007/s11223-013-9496-4.

Daouadji, T.H. (2017), "Analytical and numerical modeling of interfacial stresses in beams bonded with a thin plate", *Adv. Comput. Des.*, **2**(1), 57-69. https://doi.org/10.12989/acd.2017.2.1.057.

Daouadji, T.H., Abbès, B., Bensatallah, T. and Abbès, F. (2025a), "Analysis of interface sliding in a

composite I-steel-concrete beam reinforced by a composite material plate: The effect of concrete-steel connection modes", *J. Compos. Sci.*, **9**(6), 273. https://doi.org/10.3390/jcs9060273.

Daouadji, T.H., Abbès, F., Bensatallah, T. and Abbès, B. (2025b), "Analytical and numerical investigation of adhesive-bonded T-shaped steel-concrete composite beams for enhanced interfacial performance in civil engineering structures", *Invent.*, **10**(4), 61. https://doi.org/10.3390/inventions10040061.

Daouadji, T.H., Benferhat, R., Abbes, B., Rabahi, A., Bensatallah, T. and Abbes, F. (2025c), "Mechanical behavior of steel-concrete composite boxes reinforced with composite materials: Analysis and modeling", *Struct. Eng. Mech.*, **95**(5), 341-355. https://doi.org/10.12989/sem.2025.95.5.341.

Daouadji, T.H., Rabahi, A., Abbes, B. and Adim, B. (2016), "Theoretical and finite element studies of interfacial stresses in reinforced concrete beams strengthened by externally FRP laminates plate", *J. Adhes. Sci. Technol.*, **30**(12), 1253-1280. https://doi.org/10.1080/01694243.2016.1140703.

Ghelamallah, R., Rabia, B., Youcef, T. and Tahar, H.D. (2025), "Vibration analysis of FG beams with a new type of gradient variation reposed on elastic foundations", *Struct. Eng. Mech.*, **95**(4), 327-340. https://doi.org/10.12989/sem.2025.95.4.327.

Henni, A.H. and Daouadji, T.H. (2025a), "Application of a new improved Airy polynomial function for FGM cantilever beams under concentrated load", *Couple. Syst. Mech.*, **14**(2), 183-195. https://doi.org/10.12989/csm.2025.14.2.183.

Henni, A.H. and Daouadji, T.H. (2025b), "Analysis and modeling of the behavior of exponentially graded cantilever beams loaded by various parabolic distribution loads", *Struct. Eng. Mech.*, **95**(1), 43-50. https://doi.org/10.12989/sem.2025.95.1.043.

Jiang, R., Wu, Q., Xiao, Y., Peng, M., Au, F.T.K., Xu, T. and Chen, X. (2023), "The shear lag effect of composite box girder bridges with corrugated steel webs", *Struct.*, **48**, 1746-1760. https://doi.org/10.1016/j.istruc.2023.01.031.

Lee, D.H., Oh, J.Y., Kang, H., Kim, K.S., Kim, H.J. and Kim, H.Y. (2015), "Structural performance of prestressed composite girders with corrugated steel plate webs", *J. Constr. Steel Res.*, **104**, 9-21. https://doi.org/10.1016/j.jcsr.2014.09.014.

Ljubinković, F., Martins, J.P., Gervásio, H., da Silva, L.S. and Pedro, J.O. (2019), "Experimental behavior of curved bottom flanges in steel box-girder bridge decks", *J. Constr. Steel Res.*, **160**, 169-188. https://doi.org/10.1016/j.jcsr.2019.05.031.

Pathirana, S.W., Uy, B., Mirza, O. and Zhu, X. (2015), "Strengthening of existing composite steel-concrete beams utilising bolted shear connectors and welded studs", *J. Constr. Steel Res.*, **114**, 417-430. https://doi.org/10.1016/j.jcsr.2015.09.006.

Rabia, B., Daouadji, T.H. and Abderezak, R. (2023), "Mechanical behavior of RC beams bonded with thin porous FGM plates: Case of fiber concretes based on local materials from the mountains of the Tiaret highlands", *Couple. Syst. Mech.*, **12**(3), 241-260. https://doi.org/10.12989/csm.2023.12.3.241.

Rabia, B., Tahar, H.D., Boussad, A., Tayeb, B., Abderezak, R. and Fazilay, A. (2025), "Analytical and numerical study of composite twin-girder bridge decks with adhesive connectors and composite reinforcement", *Couple. Syst. Mech.*, **14**(4), 327-345. https://doi.org/10.12989/csm.2025.14.4.327.

Shi, F., Wang, D. and Chen, L. (2021), "Study of flexural vibration of variable cross-section box-girder bridges with corrugated steel webs", *Struct.*, **33**, 1107-1118. https://doi.org/10.1016/j.istruc.2021.05.004.

Szewczyk, P. (2024), "Experimental and numerical study of steel-concrete composite beams strengthened under load", *Mater.*, **17**(18), 4510. https://doi.org/10.3390/ma17184510.

Tayeb, B., Abderezak, R. and Daouadji, T.H. (2024), "Mechanical behavior of composite beam aluminum-sandwich honeycomb strengthened by imperfect FGM plate under thermo-mechanical loading", *Couple. Syst. Mech.*, **13**(2), 133-151. https://doi.org/10.12989/csm.2024.13.2.133.

Tayeb, B., Daouadji, T.H., Abderezak, R. and Tounsi, A. (2021), "Structural bonding for civil engineering structures: New model of composite I-steel-concrete beam strengthened with CFRP plate", *Steel Compos. Struct.*, **41**(3), 417-435. https://doi.org/10.12989/scs.2021.41.3.417.

Tounsi, A. (2006), "Improved theoretical solution for interfacial stresses in concrete beams strengthened with FRP plate", *Int. J. Solid. Struct.*, **43**(14-15), 4154-4174. https://doi.org/10.1016/j.ijsolstr.2005.03.074.

Tounsi, A., Daouadji, T.H. and Benyoucef, S. (2008), "Interfacial stresses in FRP-plated RC beams: Effect of adherend shear deformations", *Int. J. Adhes. Adhesiv.*, **29**, 313-351. https://doi.org/10.1016/j.ijadhadh.2008.06.008.

Wang, X., Miao, C. and Wang, X. (2021), "Prediction analysis of deflection in the construction of composite box-girder bridge with corrugated steel webs based on MEC-BP neural networks", *Struct.*, **32**, 691-700. https://doi.org/10.1016/j.istruc.2021.03.011.

Yan, W.T., Han, B., Xie, H.B., Li, P.F. and Zhu, L. (2020), "Research on numerical model for flexural behaviors analysis of precast concrete segmental box girders", *Eng. Struct.*, **219**, 110733. https://doi.org/10.1016/j.engstruct.2020.110733.

Zhang, Z., Zou, P., Deng, E.F., Ye, Z., Tang, Y. and Li, F.R. (2023), "Experimental study on prefabricated composite box girder bridge with corrugated steel webs", *J. Constr. Steel Res.*, **201**, 107753. https://doi.org/10.1016/j.jcsr.2022.107753.

Zhu, Y., Chen, L., Huang, G., Wang, J., Fu, S. and Bai, Y. (2025), "Intelligent design of steel-concrete composite box girder bridge cross-sections based on generative models", *Auto. Constr.*, **176**, 106292. https://doi.org/10.1016/j.autcon.2025.106292.